

4300 to 3500 calendar yr B.C. (10), a finding that is consistent with our pollen data.

A single *Manihot* sp. pollen grain found in SAV4 dates to about 4600 calendar yr B.C. The surface morphology and large size (at least 150 μm) of the grain (Fig. 4C) indicate that it is probably from domesticated manioc (*Manihot esculentum*), although the species cannot be positively identified from the pollen. Manioc is an insect-pollinated plant, and its pollen is rare in sediments. Thus, either the discovery of *Manihot* sp. at San Andrés was fortuitous, or abundant stands of *Manihot* sp. were growing close to the site. Its occurrence correlates with the period of maximum burning and land clearance by farmers at San Andrés.

By about 3400 calendar yr B.C., the barrier beach and lagoon system had migrated northward, and the lagoon began to fill with sand, silt, and clay typical of distributary channel levees in the Grijalva deltaic system (5). Floral and faunal data from all excavations and cores confirm that the levee bordered a brackish estuary. Present were brackish gastropods (*Nassarius vibex* and *Nerita reclinata*), marsh clam (*Rangia cuneata*), oysters (*Ostrea* sp.), garfish (*Lepisosteus* spp.), and manatee (*Trichechus manatus*), as well as abundant red mangrove. Radiocarbon analyses (Table 1) confirm that over 3 m of estuary sediment accumulated between 3400 and 2400 calendar yr B.C..

Human activity at San Andrés continued during estuarine deposition. The fauna noted above, except the gastropods, are mostly human food refuse. Domestic dog bones (*Canis familiaris*) are also present. Seeds and rind fragments from wild plant foods of the family Cucurbitaceae were recovered, including *Cionosicyos macranthus*, which was dated by accelerator mass spectrometry (AMS) to 2465 calendar yr B.C. (intercept date). Maize pollen is common throughout the estuary horizon in the SAV2 and SAV3 cores. Near the end of this estuarine occupation, ca. 2500 calendar yr B.C., the small *Zea* sp. pollen disappears (morphologically modern maize pollen remains), and domesticated sunflower (*Helianthus annuus*) appears. A sunflower seed and a sunflower fruit were AMS dated to 2667 calendar yr B.C. and 2548 calendar yr B.C., respectively (intercept dates) (Table 1). These are the earliest known examples of a fully domesticated sunflower (11). This discovery suggests that the theories pertaining to the origin of the domesticated sunflower in the eastern United States (12) now need revision. Cotton (*Gossypium* sp.) pollen also appears ca. 2500 calendar yr B.C. in the SAV2 core. Its appearance with other indicators of increased agricultural activity suggests domestication, although this interpretation cannot be confirmed from the pollen alone, and wild *Gossypium* sp. does occur in the Gulf Coast region farther to the east (13).

The earliest direct (AMS) dates on maize cobs in Mexico are ca. 4300 calendar yr B.C.

(5400 yr B.P.) from highland Oaxaca (14). Analyses of these fully domesticated maize cobs and similar early cobs from highland Tehuacán confirm that domestication must have occurred before 4000 calendar yr B.C. (10). Our pollen evidence from Tabasco suggests that initial maize domestication occurred at least 1000 years earlier (i.e., before 5000 calendar yr B.C.). The occurrence of *Manihot* sp. at San Andrés indicates indirect contact with farmers in the Amazon basin, where DNA evidence suggests that manioc was domesticated (15). Such an early appearance of maize and manioc in lowland Tabasco adds support for the proposed origin of New World agriculture in a humid tropical setting, and for the early exchange of cultigens between Mesoamerica and lowland regions of Central and South America (14, 16, 17).

References and Notes

1. R. S. MacNeish, in *The Prehistory of the Tehuacan Valley*, vol. 1, D. S. Byers, Ed. (Univ. of Texas Press, Austin, TX, 1967), pp. 290–309.
2. R. S. MacNeish, M. W. Eubanks, *Lat. Am. Antiq.* 11, 3 (2000).
3. M. D. Coe, R. A. Diehl, *In the Land of the Olmec*, vol. 1 of *The Archaeology of San Lorenzo Tenochtitlan* (Univ. of Texas Press, Austin, TX, 1980).
4. R. González Lauck, in *Los olmecas en Mesoamérica*,

- J. E. Clark, Ed. (El Equilibrista, Mexico, and Turner Libros, Madrid, 1994), pp. 93–111.
5. B. G. Thom, *J. Ecol.* 55, 301 (1967).
6. W. F. Rust III, B. W. Leyden, in *Corn and Culture in the Prehistoric New World*, S. Johannessen, C. A. Hastorf, Eds. (Westview Press, Boulder, CO, 1994), pp. 181–201.
7. M. D. Pohl et al., *Lat. Am. Antiq.* 7, 355 (1996).
8. D. R. Whitehead, E. J. Langham, *Bull. Torrey Bot. Club* 99, 7 (1965).
9. J. Doebley, *Econ. Bot.* 44 (suppl. 3), 6 (1990).
10. B. F. Benz, *Proc. Natl. Acad. Sci. U.S.A.* 98, 2104 (2001).
11. D. L. Lentz, M. D. Pohl, K. O. Pope, A. R. Wyatt, *Econ. Bot.*, in press.
12. B. D. Smith, *The Emergence of Agriculture* (Scientific American Library, New York, 1998).
13. J. D. Sauer, *Historical Geography of Crop Plants: A Selective Roster* (CRC Press, London, 1993).
14. D. R. Piperno, K. V. Flannery, *Proc. Natl. Acad. Sci. U.S.A.* 98, 2101 (2001).
15. K. M. Olsen, B. A. Schaal, *Proc. Natl. Acad. Sci. U.S.A.* 96, 5586 (1999).
16. D. R. Piperno, D. M. Pearsall, *The Origins of Agriculture in the Lowland Neotropics* (Academic Press, San Diego, CA 1998).
17. D. R. Piperno et al., *Nature* 407, 894 (2000).
18. M. Stuiver, P. J. Reimer, R. Reimer, CALIB radiocarbon calibration. Program software is available at <http://depts.washington.edu/qil/calib/>.
19. Funded by grants from the Archaeology Program of NSF (grant BCS-9617389) and from the Foundation for the Advancement of Mesoamerican Studies, Inc. We thank the Mexican Instituto Nacional de Antropología e Historia, especially R. González Lauck, and The New World Archaeological Foundation, Brigham Young University, Provo, UT.

28 February 2001; accepted 6 April 2001

Role of Rab9 GTPase in Facilitating Receptor Recruitment by TIP47

Kate S. Carroll, John Hanna, Iris Simon,* Jeff Krise, Pierre Barbero, Suzanne R. Pfeffer†

Mannose 6-phosphate receptors (MPRs) deliver lysosomal hydrolases from the Golgi to endosomes and then return to the Golgi complex. TIP47 recognizes the cytoplasmic domains of MPRs and is required for endosome-to-Golgi transport. Here we show that TIP47 also bound directly to the Rab9 guanosine triphosphatase (GTPase) in its active, GTP-bound conformation. Moreover, Rab9 increased the affinity of TIP47 for its cargo. A functional Rab9 binding site was required for TIP47 stimulation of MPR transport in vivo. Thus, a cytosolic cargo selection device may be selectively recruited onto a specific organelle, and vesicle budding might be coupled to the presence of an active Rab GTPase.

Mannose 6-phosphate receptors (MPRs) deliver newly synthesized lysosomal hydrolases from the Golgi complex to prelysosomes and then return to the trans-Golgi network (TGN) to pick up more cargo (1, 2). Export of MPRs from the Golgi is mediated by the AP-1 adaptor complex, which binds MPR cytoplas-

mic domains and recruits these receptors into clathrin-coated vesicles. MPR transport from endosomes to the Golgi is mediated by a protein named TIP47 (tail-interacting protein of 47 kD) that binds to a different signal in MPR cytoplasmic domains and is required for their recycling to the Golgi both in vitro and in vivo (3). Finally, MPR endocytosis is mediated by the AP-2 clathrin adaptor at the plasma membrane (1, 2).

A fundamental question in cell biology is how a single receptor is recognized by different transport machineries depending on its intracellular location. One possibility is that

Department of Biochemistry, Stanford University School of Medicine, Stanford, CA 94305-5307, USA.

*Present address: Eos Biotechnology Inc., South San Francisco, CA 94080.

†To whom correspondence should be addressed. E-mail: pfeffer@cmgm.stanford.edu

REPORTS

organelle-specific proteins corecruit cytosolic, cargo-packaging proteins to a particular organelle. Because Rab proteins are located on distinct membrane-bound compartments, we tested the possibility that TIP47 was recruited selectively onto late endosomes because of the combined presence of both a specific Rab GTPase and MPR cytoplasmic domains.

The Rab9 GTPase is localized predominantly to late endosomes, and like TIP47, it is also required for MPR transport from endosomes to the Golgi complex (4, 5). We first tested whether TIP47 could interact with

Rab9. Partially purified, cytosolic TIP47 (6) bound to His-tagged Rab9-GTP in preference to His-tagged Rab9-GDP (Fig. 1A). Binding was specific: addition of a twofold excess of Rab9 protein that was not tagged with His could compete for binding, whereas excess untagged Rab7 GTPase could not (8). Rab7 is the closest relative of Rab9 [57% identical (4, 9)] and functions in late endosome fusion (10), a process that does not appear to involve TIP47.

To ensure that the binding of cytosolic TIP47 to Rab9 was direct, we repeated the binding experiments using recombinant

TIP47 protein. Recombinant, His-tagged TIP47 bound directly to Rab9 and showed some preference for the GTP-bound form of the Rab9 GTPase (Fig. 1B). Indeed, binding studies using NH₂-terminal truncations revealed that TIP47 residues 152 to 187 were important for Rab9 binding (Fig. 1C). These residues are distinct from those that make up the MPR cytoplasmic domain binding site near TIP47's COOH-terminus (3).

If membrane-associated, native Rab9 is important for TIP47-membrane association, TIP47 binding capacity should decrease if Rab9 is depleted from membranes. To deplete Rab9, we used Rab GDI, which binds prenylated Rabs under specific conditions and removes them from membranes (11). Significant amounts of TIP47 bound to endosome-enriched membranes (Fig. 1D). After a brief pretreatment with increasing amounts of purified Rab GDI, the level of Rab9 present on the membranes could be decreased significantly. Concomitantly, TIP47 binding capacity was also decreased (Fig. 1D). Under conditions where we could deplete membranes of all detectable Rab9, a fraction of TIP47 remained membrane-associated. It is likely that the remaining protein was associated with endosomes via its interaction with MPR cytoplasmic domains (3).

We next tested whether recombinant TIP47 could interact concomitantly with the cytoplasmic domain of the cation-independent (CI-) MPR and Rab9. Recombinant TIP47 was retained on glutathione-Sepharose by its direct interaction with the cytoplasmic domain of the CI-MPR [fused to glutathione-S-transferase (GST), Fig. 2A]. Rab9 does not bind the CI-MPR. However, if a ternary complex formed between the CI-MPR, TIP47, and Rab9, Rab9 would be retained on the glutathione-Sepharose resin in a TIP47-dependent manner. Indeed, Rab9 bound to immobilized CI-MPR only in the presence of TIP47 in a concentration-dependent manner (Fig. 2A). Thus TIP47 formed a ternary complex linking the CI-MPR and Rab9.

Quantitative evaluation of this immunoblot data (Fig. 2B) revealed that TIP47 bound more tightly to the CI-MPR cytoplasmic domain when Rab9 was present. The data were fit to a curve corresponding to an apparent K_d of 0.3 μ M, a value that is one-third that obtained for TIP47:MPR interaction in the absence of Rab9 [1 μ M (7)]. This difference was confirmed using an entirely different solution-binding assay using fluorescently labeled TIP47 (Fig. 2C). Thus, Rab9 enhanced the interaction of TIP47 with the CI-MPR at least threefold.

Conversely, the CI-MPR also enhanced the association of TIP47 and Rab9. As expected, in the absence of the CI-MPR cytoplasmic domain, Rab9 bound to His-tagged TIP47 (Fig. 3A). Moreover, the amount of

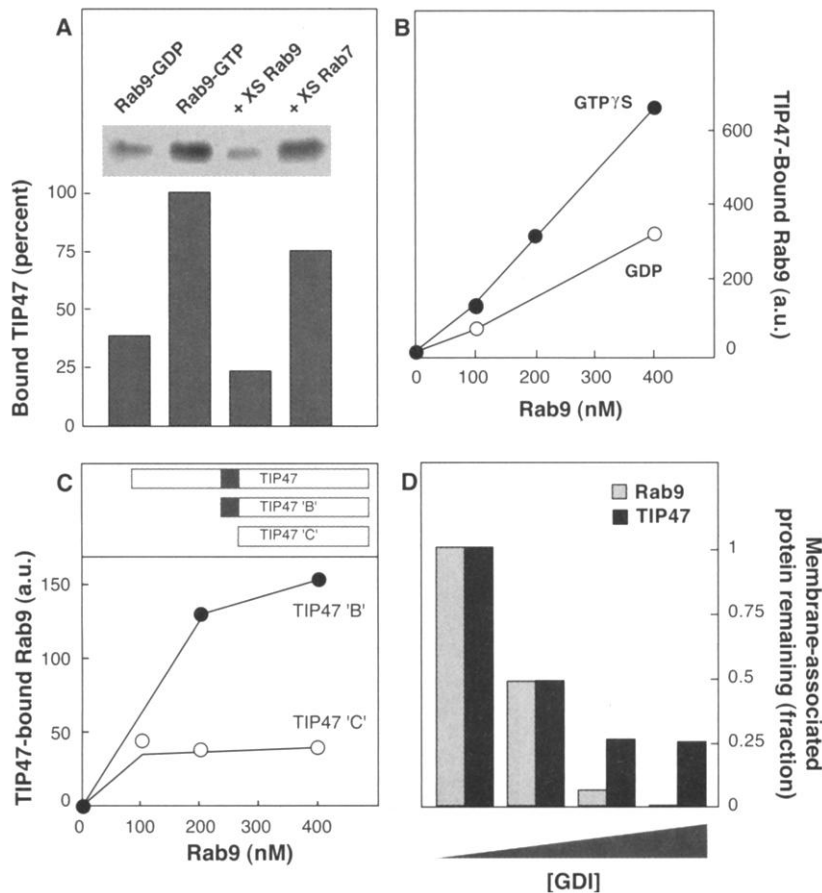


Fig. 1. TIP47 binds Rab9-GTP specifically. (A) His-Rab9 wild-type (50 μ g; "Rab9-GDP") or His-Rab9 Q66L (50 μ g; "Rab9-GTP") was incubated in the presence of either 5 μ M GDP or GTP, respectively, with highly enriched cytosolic TIP47 for 2 hours at room temperature in binding buffer (25 mM Tris pH 7.5, 150 mM NaCl, 5 mM MgCl₂, 12 mM imidazole). Ni-NTA-agarose slurry (35 μ l, Pharmacia) was added for 30 min; beads were collected, washed 3 times with 1.5 ml buffer + 0.1% CHAPS, eluted with 100 mM EDTA, and analyzed by SDS-polyacrylamide gel electrophoresis (12%). TIP47 was detected by immunoblot analysis. Where indicated, non-His-tagged, Rab9 wild-type (100 μ g) or Rab7 (100 μ g) proteins were included with His-Rab9-GTP in the reactions (+ XS Rab9, +XS Rab7). (B) TIP47 polypeptide recognizes Rab9-GTP. Rab9 protein was preincubated with 50 μ M GDP or GTP γ S for 80 min. Pure, recombinant His-TIP47 (100 nM) in 50 μ M nucleotide, 10 μ g/ml bovine serum albumin (BSA), was then added for 60 min at 37°C. Complexes were analyzed by immunoblot using antibodies against Rab9. (C) TIP47 residues 152 to 187 are necessary for Rab9 binding. Proteins were purified and binding determined as in (B); constructs 'B' and 'C' comprise residues 152 to 434 or 188 to 434, respectively, and are fully active in MPR binding. (D) TIP47 binding to endosome membranes is dependent on membrane-bound Rab9. Endosome-enriched membranes were pretreated with pure bovine brain GDI to remove Rab9 as described (18). Binding of recombinant TIP47 (50 nM) was then determined by incubation with 3 μ g membranes, in 0.1 mg/ml BSA and 0.1 mM GTP γ S for 5 min at 37°C. The amount of bound TIP47 or membrane-associated Rab9 was determined by immunoblot. The pairs of bars shown reflect reactions containing membranes pretreated with 0, 100, 120, or 160 μ g/ml GDI for 5 min at 37°C.

REPORTS

Rab9 that was bound to TIP47 increased significantly upon addition of increasing amounts of the CI-MPR cytoplasmic domain (Fig. 3A). The presence of Rab9 in the eluted complexes was absolutely dependent on the presence of TIP47. Thus both Rab9 and the CI-MPR cytoplasmic domain enhanced each other's interaction with TIP47.

Because TIP47 is likely to be involved in transport vesicle formation, it was possible that TIP47 recruited Rab9 into transport vesicles coupled with its conversion to an active, GTP-bound form. However, nucleotide dissociation, as monitored by the ability of Rab9 to bind GTP γ ³⁵S after GDP release, was unchanged in the presence of TIP47. Thus, cytosolic TIP47 does not appear to be a nucleotide exchange rate-enhancer for Rab9.

TIP47 function in vivo required TIP47's capacity to bind Rab9 efficiently. When TIP47 residues Ser¹⁶⁷ValVal were mutated to Ala¹⁶⁷AlaAla, the ability of recombinant TIP47 to bind Rab9 in vitro was decreased to about one-fifth (Fig. 3B). Cells transfected with wild-type TIP47, but not mutant TIP47, showed an increase in transport of MPRs from endosomes to the TGN (12, 13); indeed, the mutant was inhibitory at comparable expression levels.

TIP47 represents a Rab9 effector that binds with preference to Rab9-GTP. Furthermore, the binding of Rab9 enhances the interaction of TIP47 with MPR cytoplasmic domains. Thus, Rab9 is likely to enhance the endosome-recruitment of TIP47 as well as the cargo capture process.

We have shown that Rab9 increases the affinity of TIP47 for the CI-MPR: the K_d decreases from 1 μ M to 300 nM. This modulation may be critical for TIP47 function. TIP47 binds to the CI-MPR with an affinity of 1 μ M (7). Given its presence in cytosol at ~300 nM, if TIP47 used only the MPR for membrane binding, ~10% would be membrane-associated, but without any organelle specificity. Using Rab9 as an organelle-specific coreceptor, the K_d for TIP47 binding to MPRs decreases to the cytosolic concentration of TIP47. In this scenario, 50% of TIP47 should be membrane-associated, and all of that should be associated with endosomes; this is close to the ratio we observe (3). Thus, an endosome-specific Rab protein triggers the organelle-specific recruitment of TIP47 that might otherwise bind MPRs when they are present in other compartments. In addition, the low intrinsic affinity of TIP47 for MPRs also decreases its binding to MPRs located in compartments where the receptors should interact with other cargo selection devices.

Because Rab9-GTP enhances TIP47 endosome association and cargo binding, it appears to function during transport vesicle for-

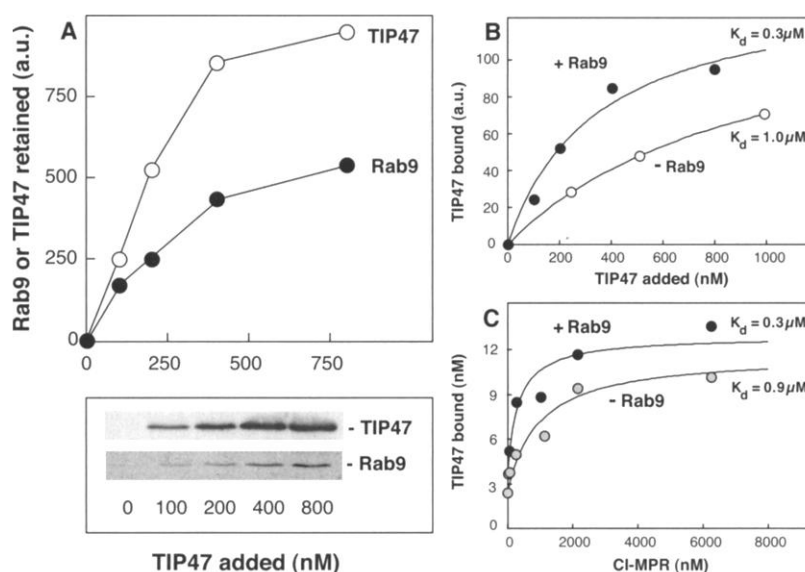


Fig. 2. (A) TIP47 binds both CI-MPR and Rab9 in a ternary complex. GST-CI-MPR (100 nM) was mixed with TIP47 in binding buffer without imidazole plus 100 μ M GTP, 10 μ g/ml BSA; reactions also contained Rab9 (100 nM) in 300 μ l. Binding was for 60 min at 37°C. Complexes were collected after addition of 40 μ l glutathione-Sepharose (50% slurry) for 30 min at 20°C, 3 washes, and two elutions with 50 μ l, 20 mM glutathione. The amount of bound Rab9 and TIP47 was determined by immunoblot followed by densitometric scanning. Blots in the lower panel were scanned to yield the upper panel curves. (B) Rab9 enhances TIP47:MPR interaction. Data from (A) were fit to a binding isotherm to obtain a K_d estimate of 0.3 μ M (filled circles). These data are compared with values obtained in the absence of Rab9 (averages of triplicates, open circles) using a fluorescence assay (7), which fit a curve corresponding to $K_d = 1 \mu$ M. (C) Fluorescent TIP47 binding assay. Reactions contained: Texas Red TIP47 (10 nM active protein), 1.5 μ M Rab9 (where indicated), 100 μ M GTP, and increasing amounts of GST-CI-MPR in 50 mM Hepes, 150 mM KCl, 1 mM MgCl₂, 10% glycerol, 0.6 mg/ml BSA (7). Reactions were at 37°C for 60 min; glutathione-Sepharose slurry was added for another 30 min at room temperature. Resin was washed with 1 ml buffer and eluted in 0.5 ml, 20 mM glutathione. Backgrounds were not subtracted and are accounted for in the curve fits.

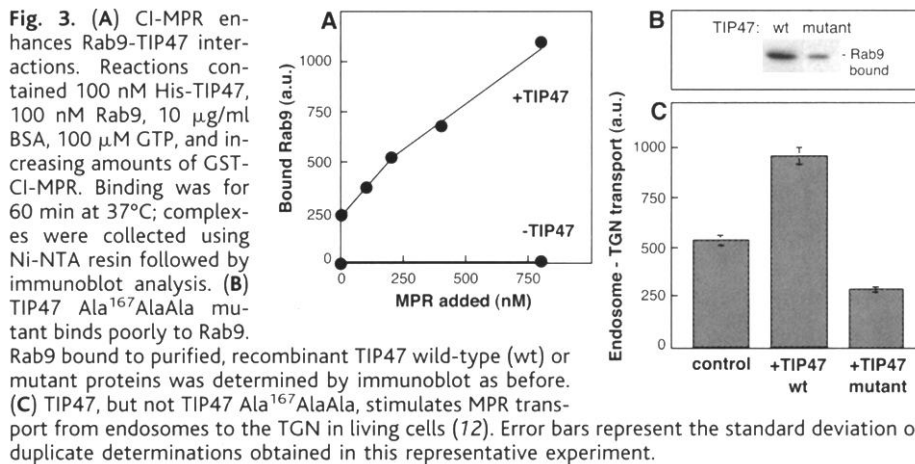


Fig. 3. (A) CI-MPR enhances Rab9-TIP47 interactions. Reactions contained 100 nM His-TIP47, 100 nM Rab9, 10 μ g/ml BSA, 100 μ M GTP, and increasing amounts of GST-CI-MPR. Binding was for 60 min at 37°C; complexes were collected using Ni-NTA resin followed by immunoblot analysis. (B) TIP47 Ala¹⁶⁷AlaAla mutant binds poorly to Rab9. Rab9 bound to purified, recombinant TIP47 wild-type (wt) or mutant proteins was determined by immunoblot as before. (C) TIP47, but not TIP47 Ala¹⁶⁷AlaAla, stimulates MPR transport from endosomes to the TGN in living cells (12). Error bars represent the standard deviation of duplicate determinations obtained in this representative experiment.

matation. In addition, GTP-bearing Rabs recruit cytosolic docking factors to the surfaces of transport vesicles to facilitate SNARE pairing before fusion (14, 15). Thus Rabs are likely to function in both vesicle formation and docking (16, 17).

Our data support a model in which Rab9 facilitates the recruitment of TIP47 onto MPR-containing endosomes, rather than onto other membrane-bound compartments that may also contain MPRs. Rab9 is likely to

stimulate cargo capture by enhancing the affinity with which TIP47 binds to receptor cargo. After vesicle formation, Rab9 may also participate in the process by which transport vesicles dock with their specific, corresponding target.

References and Notes

1. S. Kornfeld, *Annu. Rev. Biochem.* **61**, 307 (1992).
2. _____, I. Mellman, *Annu. Rev. Cell Biol.* **5**, 483 (1989).
3. E. Diaz, S. R. Pfeffer, *Cell* **93**, 433 (1998).

4. D. Lombardi, et al. *EMBO J.* **12**, 677 (1993).
5. M. A. Riederer, T. Soldati, A. D. Shapiro, J. Lin, S. R. Pfeffer, *J. Cell Biol.* **125**, 573 (1994).
6. His-tagged TIP47 was purified after expression in *Escherichia coli* (3); 10% glycerol was added. GST-CI-MPR cytoplasmic domain and TIP47 constructs, and antibodies against TIP47 were as described (3). Texas Red sulfonfyl chloride (Molecular Probes, Eugene, Oregon), was covalently attached to TIP47 and used for binding as described (7). Cytosolic TIP47 was purified from bovine kidney cytosol (3.6 g) by chromatography on Fast Flow Q-Sepharose (18 ml), eluted with 0 to 400 mM NaCl in 25 mM Tris pH 7.5. Fractions were dialyzed into 10 mM Na phosphate pH 7.5 and applied onto a hydroxyapatite column (7 ml), eluted with a Na phosphate gradient at pH 7.5. Purification for Fig. 1A included an additional anion exchange step at pH 6.8. This material is 150-fold enriched for TIP47.
7. J. P. Krise, P. M. Sincok, J. G. Orsel, S. R. Pfeffer. *J. Biol. Chem.* **275**, 25188 (2000).
8. For Rab9-GTP we utilized Rab9 CLLL, which is a wild-type protein with an altered COOH-terminus, to

- enhance stability upon expression in *E. coli*. The protein shows entirely wild-type nucleotide binding properties, becomes mono-geranylgeranylated in vitro, and can support in vitro transport of the CI-MPR. Rab9 Q66L was used in Fig. 1 only; this protein was generated by polymerase chain reaction mutagenesis and is defective in nucleotide hydrolysis, favoring the GTP-bound state.
9. P. Chavrier, M. Vingron, C. Sander, K. Simons, M. Zerial, *Mol. Cell Biol.* **10**, 6578 (1990).
10. Y. Feng, B. Press, A. Wandinger-Ness, *J. Cell Biol.* **131**, 1435 (1995).
11. F. Schimmöller, I. Simon, S. R. Pfeffer. *J. Biol. Chem.* **273**, 22161 (1998).
12. Plasmids encoding 3XMyC-TIP47 or 3Xmyc-TIP47 Ala¹⁶⁷AlaAla were transiently transfected into cells stably expressing a CD-MPR that contains a tyrosine sulfation site to enable monitoring of endosome-to-TGN transport in vivo (13). Transport was measured 43 hours after Eugene (Roche Diagnostics, Indianapolis) transfection as described (13). Data were corrected for the efficiency of transfection (36%), which was determined in parallel by immunofluorescence

- microscopy using cells transfected with a plasmid encoding green fluorescent protein.
13. C. Itin, C. Rancano, Y. Nakajima, S. R. Pfeffer, S. R. *J. Biol. Chem.* **272**, 27737 (1997).
14. S. R. Pfeffer, *Nature Cell Biol.* **1**, E17 (1999).
15. P. Novick, M. Zerial, *Curr. Opin. Cell Biol.* **9**, 496 (1997).
16. G. Jedd, J. Mulholland, N. Segev, *J. Cell Biol.* **137**, 563 (1997).
17. H. McLauchlan et al., *Curr. Biol.* **8**, 34 (1998).
18. T. Soldati, M. A. Riederer, S. R. Pfeffer, *Mol. Biol. Cell* **4**, 425 (1993).
19. Research was supported by a research grant (DK37332) from the National Institutes of Health; I.S. and J.K. were postdoctoral fellows of the Deutsche Forschungsgemeinschaft and the Pharmaceutical Research and Manufacturers of America Foundation, respectively; K.S.C. was a predoctoral trainee of NIH. We thank L. Ding and B. O'Connor for contributions to the identification of the Rab9 binding site.

23 October 2000; accepted 19 March 2001

A GDP/GTP Exchange Factor Involved in Linking a Spatial Landmark to Cell Polarity

Pil Jung Kang, Anthony Sanson, Bongyong Lee, Hay-Oak Park*

In both animal and yeast cells, signaling pathways involving small guanosine triphosphatases (GTPases) regulate polarized organization of the actin cytoskeleton. In the budding yeast *Saccharomyces cerevisiae*, the Ras-like GTPase Bud1/Rsr1 and its guanosine 5'-diphosphate (GDP)/guanosine 5'-triphosphate (GTP) exchange factor Bud5 are involved in the selection of a specific site for growth, thus determining cell polarity. We found that Bud5 is localized at the cell division site and the presumptive bud site. Its localization is dependent on potential cellular landmarks, such as Bud3 and Axl2/Bud10 in haploid cells and Bud8 and Bud9 in diploid cells. Bud5 also physically interacts with Axl2/Bud10, a transmembrane glycoprotein, suggesting that a receptor-like transmembrane protein recruits a GDP/GTP exchange factor to connect an intrinsic spatial signal to oriented cell growth.

Yeast cells undergo oriented cell division by choosing a specific bud site on the cell cortex. Haploid **a** and α cells bud in an axial pattern in which both mother and daughter cells select a bud site immediately adjacent to their previous division site. Diploid **a**/ α cells bud in a bipolar pattern: Mother cells select a bud site adjacent to their daughter or on the opposite end of the cell, whereas daughter cells always choose a bud site directed away from their mother (1–3). The axial pattern appears to depend on a transient cortical marker that may involve proteins such as septins, Bud3, Bud4, and Axl2 (4–12). The bipolar budding pattern appears to depend on persistent markers that are deposited at both poles of the cell. The genes that are specifically required for the bipolar pattern may encode or regulate the bipolar cortical cues (4, 13). A key

issue in understanding the mechanism of polarity establishment is to determine how these potential landmarks are linked to the intracellular signaling pathways. A likely candidate that links these spatial cues to polarity establishment is the Bud1 GTPase module, which is composed of Bud1, its GTPase-activating protein (GAP) Bud2, and Bud5 (3, 4, 14–18). These proteins are required for both axial and bipolar budding patterns.

To examine Bud5 localization, we used a functional chromosomal *BUD5-GFP* (GFP, green fluorescent protein) fusion. Several aspects of the Bud5-GFP localization in haploid **a** and α cells were notable (Fig. 1A) (19). Bud5-GFP was present in a small patch in unbudded cells. After bud emergence, Bud5-GFP localized throughout the periphery of the bud. As the bud continued to grow, the Bud5-GFP signal at the bud periphery diminished, and the signal was observed as a double ring encircling the mother-bud neck. Following cytokinesis, a single ring of Bud5-GFP persisted in both mother

and newly born daughter cells. The Bud5-GFP ring then disappeared, and Bud5-GFP concentrated in a patch at the incipient bud site. Calcofluor staining of bud scars confirmed that the ring of Bud5-GFP localized at the division site and a new patch of Bud5-GFP appeared next to the previous division site (Fig. 1A). Thus, Bud5-GFP localized to the cell division site and the presumptive bud site, and its localization changed over the cell cycle. The localization of Bud5-GFP in haploid cells overlapped extensively with that of Axl2 throughout the cell cycle and also with those of Bud3 and Bud4 during M and early G₁ phases (5–7, 12), suggesting that Bud5 may interact with these axial-specific components.

To examine whether localization of Bud5 was required for proper bud site selection, we determined the localization of Bud5-GFP and the budding pattern of haploid cells overexpressing *BUD5-GFP* from a multicopy plasmid. Bud5-GFP was often found at random locations in the cell periphery and also in the cytoplasm (Fig. 1B). These cells also exhibited partial random budding (20), suggesting that localization of Bud5 is important for proper bud site selection.

Diploid **a**/ α cells exhibit bipolar budding, as opposed to axial budding, and Bud5-GFP revealed distinct localization patterns in **a**/ α cells, particularly during G₁ and M phases (Fig. 1C) (19). Before bud emergence, Bud5-GFP was present at both poles: as a ring at one pole and in a small patch at the opposite pole. After bud emergence, Bud5-GFP localized throughout the periphery of the bud, as seen in haploid cells. At a later stage of the cell cycle, Bud5-GFP localized at the neck and at one or both poles of mother cell and bud, whereas a small percentage of cells showed a Bud5-GFP signal only at the neck. Such patterns of Bud5-GFP localization were not observed in haploid cells. Thus, localization of Bud5 to the potential bud site in **a**/ α cells before the G₁ phase was likely to contribute to the bipolar budding pattern of these cells.

Department of Molecular Genetics, The Ohio State University, Columbus, OH 43210–1292, USA.

*To whom correspondence should be addressed. E-mail: park.294@osu.edu